IOP Conference Series: Materials Science and Engineering

PAPER • **OPEN ACCESS**

Interfacial microstructure evolution of gold alloy/Sn-based solder under different thermal aging conditions

To cite this article: G Q Mu *et al* 2019 *IOP Conf. Ser.: Mater. Sci. Eng.* **504** 012008

View the article online for updates and enhancements.

This content was downloaded from IP address 117.93.176.10 on 14/10/2019 at 00:27

IOP Conf. Series: Materials Science and Engineering **504** (2019) 012008 doi:10.1088/1757-899X/504/1/012008

Interfacial microstructure evolution of gold alloy/Sn-based solder under different thermal aging conditions

G Q Mu, W Q Qu, Y C Wu and H S Zhuang

School of Mechanical Engineering and Automation, Beihang University, No.37, Xueyuan Road, Haidian District, Beijing, 100191, P.R. China

Corresponding author and e-mail: W Q Qu, quwenqing@buaa.edu.cn

Abstract. Sn-based solder is used for soldering a gold alloy and a brass sheet. Subsequently thermal aging tests are performed. The influence of thermal aging on the interfacial microstructure evolution of gold alloy/Sn-based solder and its mechanical properties was analysed. The results show that the aging time and aging temperature have large influence on the growth of interfacial compounds, and the interfacial compounds show a multiply-sublayers structure, the main components are $AuNi_2Sn_4$, $AuSn_4$, Ni_3Sn_4 and Ni_3Sn. The hardness of the interfacial compounds show a distinct layered phenomenon, in which the hardness of the first layer is the highest. Shear tests indicated that the failure happened at the gold alloy/Sn-based solder interface close to the gold alloy, showing obvious brittle fracture features. Shear strength decreases with increasing aging time at the aging temperature of 150℃ and 175℃.

1. Introduction

Gold and its alloys have many unique advantages such as high ductility, chemical stability and corrosion resistance, good thermal and electrical conductivity, and low and stable contact resistance [1]. Thus it is widely used, especially in electronic sliding contacts in highly humid or corrosive atmospheres, and for contacts with high failure costs (certain computers, communications equipment, spacecraft, and jet aircraft engines) [2-4]. However, pure gold has deficiencies such as low strength, low hardness, easy deformation, poor elasticity, and easy arcing. In order to improve the electrical contact properties of gold, gold-based alloys are often formed by adding other strengthening elements such as platinum, palladium, copper, cobalt, and nickel to gold. Au-Ni alloys, such as $AuNi_5$, $AuNi_9$, and $AuNi_9Y_{0.5}$, are commonly used as light-load open/close contacts and sliding contact materials. Among them, $AuNi_9$ alloys have higher strength and hardness, lower resistivity, excellent chemical stability, high resistance to welding and corrosion, so it is widely used [5]. In most cases, gold and its alloys must be joined with other metals. Sn-based solders usually provide the necessary electrical, mechanical and thermal connection [6].

When Sn-based solder is used to join gold alloys, the gold will rapidly dissolve into the molten Sn-based solder forming coarse, anisotropic, and brittle Au-Sn intermetallic compounds (IMC) [7-16], resulting in significant strength reduction and embrittlement of the joint. The base metal used here also contains Ni, which can also dissolve into molten Sn-based solder to form Ni-Sn intermetallic compounds. The thickness of the base metal, the soldering temperature and time, the temperature and time of solid-state thermal cycling and aging have important effects on embrittlement [17-23].The extensive investigations have been mostly carried out on the solderability of gold-plated components

Content from this work may be used under the terms of the Creative Commons Attribution 3.0 licence. Any further distribution of this work must maintain attribution to the author(s) and the title of the work, journal citation and DOI.
Published under licence by IOP Publishing Ltd

[24-31]. During the thermal aging process, the gold coating will be quickly absorbed by the Sn-based solder. Therefore, it is necessary to study the microstructure evolution of the gold alloy with a certain thickness/Sn-based solder interface during the thermal aging process.

The purpose of the present work is to clarify the interfacial microstructure evolution and its influence on mechanical property of gold alloy/Sn-based solder interface under various thermal aging conditions by means of scanning electron microscope (SEM), mechanical tests, and micro-hardness tests. This study provides a fundamental understanding for the increasing applications of gold alloys.

2. Experimental procedures

Eutectic Sn-based solder with the melting point of 183 ℃ was used to joint $AuNi_9$ alloy wire and brass sheet. The chemical composition of the $AuNi_9$ base metal is Au 91 wt% and Ni 9 wt% with a diameter of 0.5 mm, a length of 20 mm. The dimension of the brass sheet is 20 mm ×5 mm ×1 mm. The soldering process was carried out by an electric hot plate with intelligent temperature control. The lap length was 1.5mm. The solder was placed on the brass sheet, heated up to 230 ℃ until it was melted completely. The $AuNi_9$ wire was inserted into the molten solder. The soldered joints were cooled down to the room temperature.

Thermal aging test was performed at 125 ℃,150 ℃, and 175 ℃ for 4, 10, 30, 60 and 90 days. The mechanical property of the soldered joint was evaluated by shear tests at room temperature using a tensile testing machine (Instron) with a machine displacement rate of 0.5 mm/min. The average shear strength of five joints was used to investigate the mechanical properties under different aging conditions. Micro-hardness was tested by a Vickers micro-hardness tester (Mitutoyo HM-113) with 0.246 N indentation force, and 10 s holding time. The microstructure of the soldered joint was observed by a scanning electron microscope (SEM). A Hitachi S-530 SEM coupled with energy dispersive X-ray spectroscopy (EDS) was used to investigate the chemical composition of interfacial compounds (IMC) and the thickness of IMC layer presented in the soldered joints. EDS analysis and mapping were performed with an acceleration voltage of 20 kV.

3. Results and discussion

3.1. Microstructure analysis

Figure 1a shows the microstructure of the gold alloy/Sn-based solder interface before thermal aging. As shown in figure 1a, a continuous and uniform IMC is formed at the interface with a thickness of approximately 3 μm. Its composition is analyzed by EDX. The IMC layer is roughly divided into two layers: the $AuNi_2Sn_4$ phase close to the gold alloy and the $AuSn_4$+Ni_3Sn_4 phase close to the solder.

Figure 1b shows the microstructure of the gold alloy/Sn-based solder interface after 4 days dwell time at 125 ℃. It can be seen that a continuous and uniform IMC layer is formed at the interface, with a thickness of approximately 27 μm. The components of three points A, B, and C in the figure are analyzed by EDS. The results are shown in table 1. It shows that the point A close to the base metal may be $AuNi_2Sn_4$ phase, the point B close to the solder may be $AuSn_4$+Ni_3Sn_4 phase, and the light gray phase in the solder (point C) may be $AuSn_4$. According to table 1, the Ni content in the IMC layer decreases gradually as the distance from the base metal increases, and the Au content does not decrease as the distance from the base metal increases. The Au content near the solder (point C) is higher than the Au content in the IMC layer (points A and B), indicating that the diffusion rate of Au atoms in the solder is very high. The ratio of the atomic percentage of (Ni + Au) to that of Sn in point A was (43.4):(56.6), which is very close to 3:4. It is known that some binary phases in the Au–Ni–Sn ternary system [32], such as AuSn, Ni_3Sn_4 and Ni_3Sn_2, have a very high solubility of the third element, due to the similarity in the chemical and physical properties of Au and Ni. It seems that Au can enter into the Ni_3Sn_4 lattice and substitute for the Ni atoms, allowing the $AuNi_2Sn_4$ phase to form at the interface.

Figure 2a shows the microstructure of the gold alloy/Sn-based solder interface after 10 days at 150 ℃. It can be seen from the figure that a continuous and uniform layered intermetallic compound

layer is formed at the interface. The IMC layer is roughly divided into three layers. The dark gray phase close to the base metal is the first layer, the middle light gray phase is the second layer, and the dark gray phase near the solder is the third layer. By EDS analysis: the first layer is $AuNi_2Sn_4$, the middle layer is $AuSn_4$+Ni_3Sn_4, and the third layer is $AuSn_4$+Cu_6Sn_5+Ni_3Sn. After aging for 60 days, most of the $AuNi_9$ base metal has converted to intermetallic compounds. After aging for 90 days, almost all of the $AuNi_9$ base metals has converted to intermetallic compounds.

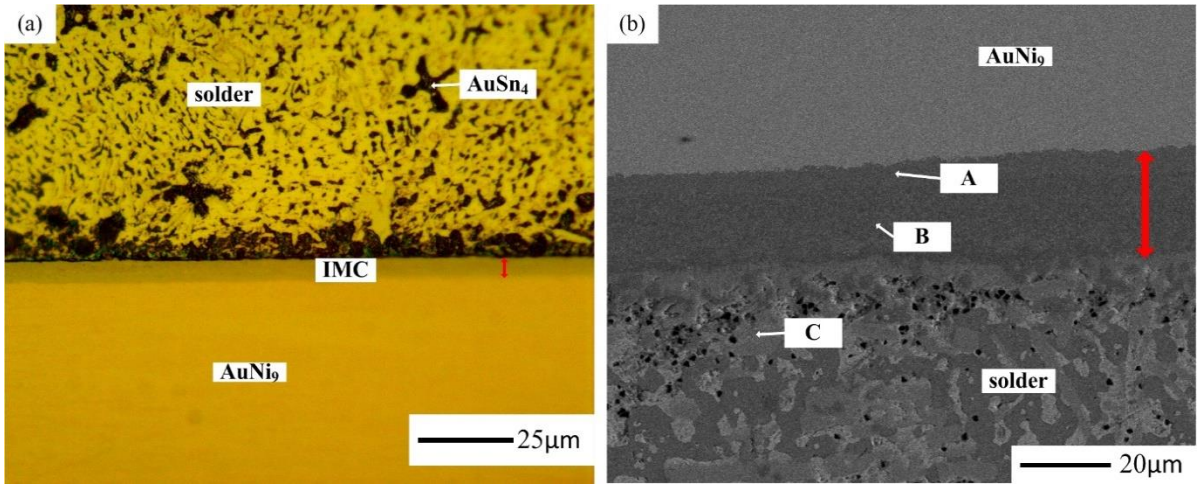

Figure 1. The microstructures of the gold alloy/Sn-based solder interface. a) Before thermal aging; b) After 4 days at 125 ℃.

Table 1. The chemical compositions of three points (as shown in figure 1b) by EDS analysis.

position	Chemical compositions (*at %*)			The posible compound phase
	Ni	Sn	Au	
A	30.18	56.58	13.23	$AuNi_2Sn_4$
B	26.31	66.25	7.44	$AuSn_4$+Ni_3Sn_4
C	0	79.70	20.30	$AuSn_4$

Figure 2b shows the microstructure of the gold alloy/Sn-based solder interface after 4 days at 175 ℃. As a whole, after aging at 175 ℃ for 4 days, the IMC layer grows significantly thicker (5.74 times of 125 ℃ for 4 days, 2.87 times of 150 ℃ for 4 days) and the solder layer becomes thinner, and the white Pb-rich phase in the IMC layer increases compared with that at 150 ℃. By EDS analysis: the dark gray phase close to the $AuNi_9$ base metal is a Ni-rich $AuNi_2Sn_4$ phase, the second layer is $AuSn_4$+Ni_3Sn_4, and a large number of white Pb-rich phase is accumulated between the compounds, and the light grey rod-shaped compound that infiltrates into the solder is $AuSn_4$. After aging for 30 days, most of the $AuNi_9$ base metal has converted to intermetallic compounds; after aging for 60 days, almost all of the $AuNi_9$ base metals has converted to intermetallic compounds.

During the thermal aging, the Au and Ni elements in the $AuNi_9$ base metal will continue to dissolve into the solder, so the thickness of the IMC layer increases. Figure 3 shows the thickness of IMC layer varying with aging time at different aging temperatures. It indicates that the thickness of the IMC layer increases with increasing aging time. At 150 ° C, the thickness of the IMC layer grows slowly before 30 days (3.23 μm/day), grows rapidly from 30 days to 60 days (14.73 μm/day), and grows slowly after 60 days (0.27 μm/day). At 175 ℃, the thickness of IMC layer grows rapidly from the initial aging period (15.4 μm/day), and it grows slowly after 30 days (1 μm/day). Before 60 days, for the same aging time, the thickness of 175 ℃ is significantly higher than that of 150 ℃. The thickness grows rapidly from 30 days at 150 ℃, but the thickness grows rapidly from initial aging period at 175 ℃. We

can see that the influence of aging temperature on thickness is bigger than aging time. The thickness of the IMC layer grows slowly in the later aging period. This is mainly due to the fact that when the aging time is longer (150 ℃ /60 d, 175 ℃ /30 d), most of the $AuNi_9$ base metal has converted to intermetallic compounds, and the solder integrates with the $AuNi_9$ base metal, so the IMC layer tends to be stable.

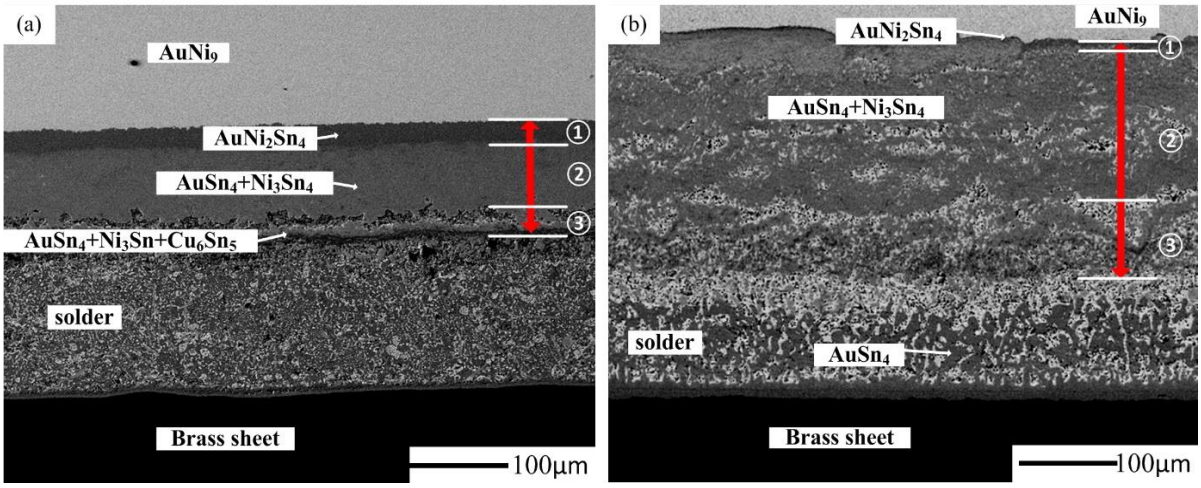

Figure 2. The microstructures of the gold alloy/Sn-based solder interface under different aging conditions. a) After 10 days at 150 ℃; b) After 4 days at 175 ℃.

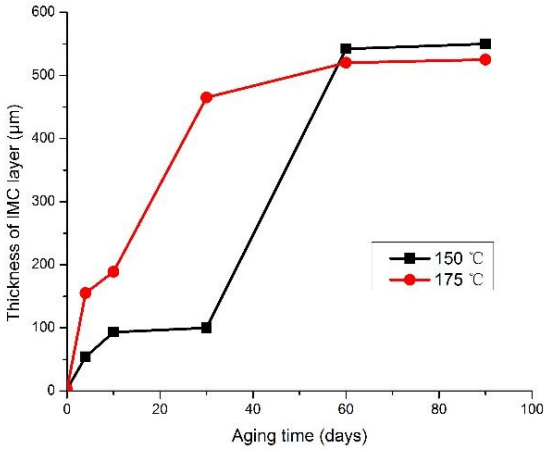

Figure 3. The thickness of IMC layer varying with aging time under different aging temperatures.

3.2. Mechanical properties

The interfacial micro-hardness was used to analyze the mechanical property. According to the interfacial microstructure, the IMC layer is roughly divided into three sublayers. The first layer consists mainly of a $AuNi_2Sn_4$ phase, the second layer mainly of $AuSn_4$+Ni_3Sn_4 phase, the third layer mainly of $AuSn_4$+Cu_6Sn_5+Ni_3Sn phase. The different composition of the IMC layer determines the different hardness levels of the IMC layer. Figure 4 shows the micro-hardness measurement of three IMC sublayers in gold alloy/Sn-based solder interface at aging temperature of 150 ℃. The figure shows that the first sublayer has the highest hardness in the range of 240-260 HV, because the composition of the first layer is mainly $AuNi_2Sn_4$ phase, the hardness of $AuNi_2Sn_4$ phase is relatively high, and the first layer is close to the $AuNi_9$ base metal, and the hardness of the $AuNi_9$ is high (tested at 271.5 HV). The hardness of the second layer is in the range of 140-160 HV, because the

composition of the second layer is mainly a mixture of $AuSn_4$, Ni_3Sn_4 and a small amount of solder, and the hardness of the solder is low (tested as 14.6 HV). The hardness of the third layer is in the range of 60-80 HV, because the composition of the third layer is mainly a mixture of $AuSn_4$, Cu_6Sn_5, Ni_3Sn and solder, and the third layer is close to the solder. During the tests, it was found that the test region was fragmented, indicating that the interfacial compounds were brittle.

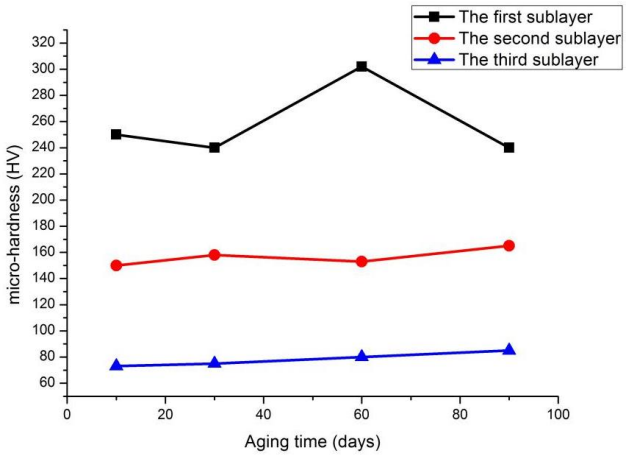

Figure 4. The micro-hardness measurement of three IMC sublayers in gold alloy/Sn-based solder interface at aging temperature of 150 ℃ for different aging time.

The microstructure reflects the effect on the mechanical properties of the soldered joints. The mechanical properties of the soldered joints before and after thermal aging were tested. The test found that the failure ocurred at the gold alloy/Sn-based solder interface close to the gold alloy, and the fracture was very smooth, showing obvious brittle fracture features, indicating that the interfacial compounds was brittle, resulting in the fracture failure of the soldered joints.

Figure 5 shows the shear strength of the soldered joints at different thermal aging conditions. From the figure, it can be seen that at the aging temperatures of 150 ℃ and 175 ℃, the shear strength decreases with the increasing aging time, which indicates that the aging time has a large influence on the mechanical properties of the soldered joints. For the same aging time, the strength at 175 ℃ is lower than that at 150 ℃, indicating that the aging temperature has a large influence on the mechanical properties of the joint. At 150 ℃, the shear strength decreased obviously when aging 10 d-30 d. At 175 ℃, the shear strength decreased when aging 0 d-30 d, and the shear strength decreased slowly after aging 30 d. Because before 30 days, the thickness of the IMC layer increased significantly and the number of interfacial brittle compounds increased, the strength decreased significantly.

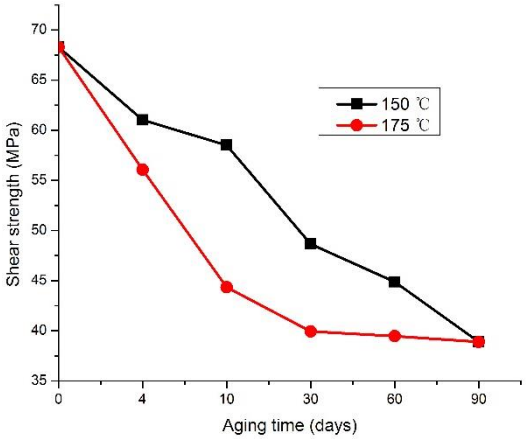

Figure 5. The shear strength of the soldered joints at different thermal aging conditions.

4. Conclusions

1) Aging time and aging temperature have large influence on the growth of interfacial compounds. Before aging and after aging at 125 ℃/4 d, the IMC layer is roughly divided into two layers: the $AuNi_2Sn_4$ layer close to the gold alloy and the $AuSn_4$+Ni_3Sn_4 layer close to the solder, the light gray rod-shaped compound in the solder is the $AuSn_4$ phase. After aging at 150 ℃/10 d and 175 ℃/4 d, the IMC layer is roughly divided into three layers: the first layer of $AuNi_2Sn_4$ phase, the second layer of $AuSn_4$+Ni_3Sn_4 phase, the third layer of $AuSn_4$+Cu_6Sn_5+Ni_3Sn phase, and the light grey rod-shaped compound in the solder is the $AuSn_4$. As the thermal aging continues, the IMC layer becomes thicker, the solder layer becomes thinner, and the white Pb-rich phase in the IMC layer and the solder layer increases.
2) The micro-hardness of the interfacial compounds shows a distinct layered phenomenon. The hardness of the first layer is the highest in the range of 240-260 HV, the hardness of the second layer is in the range of 140-160 HV, and the hardness of the third layer is in the range of 60-80 HV, mainly because of the different composition of IMC sublayer.
3) Shear tests found that the failure happened at the gold alloy/Sn-based solder interface close to the gold alloy, the fracture is very smooth, showing obvious brittle fracture features. At the aging temperatures of 150 ℃ and 175 ℃, the shear strength decreases with increasing aging time. At the same aging time, the strength at 175 ℃ is lower than that at 150 ℃.

Acknowledgement
This project was funded by key special projects of the national key R&D program (2017YFB0305700).

References

[1] Christie T, Brathwaite B 2012 Mineral Commodity Report 14-Gold, Institute of geological and nuclear sciences Ltd – Retrieved 7 June
[2] Alvarez-Berrós N L, Aide M T 2015 Global demand for gold is another threat for tropical forests. Environmental Research Letters 10(1): 014006
[3] Goodmann P 2002 Current and future uses of gold in electronics. Gold bulletin 35(1): 21-26
[4] Selig O, Siffels R, Rezus Y L A 2015 Ultrasensitive Ultrafast Vibrational Spectroscopy Employing the Near Field of Gold Nanoantennas. Physical Review Letters 114(23): 300-4
[5] Yang Y K, Tong Y P, Zhang R G, Liu J Z 2005 Development of AuNi5/CuNi20 Bimetal Rivet for Automotive Sensor[J].Electrical materials (04):3-6
[6] Laurila T, Vuorinen, Kivilahti J K 2005 Interfacial reactions between lead-free solders and common base materials. Materials Science and Engineering R; 49: 1–60
[7] Xu H, Vuorinen V, Dong H, Paulasto-Krockel M 2015 Solid-state reaction of electroplated thin film Au/Sn couple at low temperatures. Journal of Alloys and Compounds 619: 325–331
[8] Dong H, Vuorinen V, Tao X M, Laurila T, Paulasto-Krockel M 2014 Thermodynamic reassessment of Au–Cu–Sn ternary system. Journal of Alloys and Compounds; 558: 449-460
[9] Tu K N, Zeng K 2001 Tin-Lead (SnPb) solder reaction in flip chip technology. Materials Science and Engineering R; 34: 1–58
[10] Liu W, Wang C Q, Tian Y H, Chen Y R 2008 Effect of Zn addition in Sn-rich alloys on interfacial reaction with Au foils. Trans. Nonferrous Met. Soc. China 18: 617-22
[11] Chidambaram V, Hattel J, Hald J 2010 Design of lead-free candidate alloys for high-temperature soldering based on the Au–Sn system. Materials and Design 31:4638-45
[12] Arshad M K M, Jalar A, Ahmad I 2007 Characterization of parasitic residual deposition on passivation layer in electroless nickel immersion gold process. Microelectronics Reliability; 47: 1120–6
[13] Peng S P, Wu W H, Ho C E, Huang Y M 2010 Comparative study between Sn37Pb and Sn3Ag0.5Cu soldering with Au/Pd/Ni(P) tri-layer structure. Journal of Alloys and Compounds; 493: 431-7
[14] Kim P G, Tu K N 1998 Fast dissolution and soldering reactions on Au foils. Materials

Chemistry and Physics; 53:165-171
[15] Liu W, Zhang L, Hsia K J, Shang J K 2010 Fast Spreading of Liquid SnPb Solder on Gold-coated Copper Wheel Pattern. Journal of Material Science and Technology 26(12): 1143-7
[16] Massalski T B 1986 Binary alloy phase diagrams. Materials Park, OH: ASM International 316
[17] Berthou M, Retailleau P, Frémont H, Guédon-Gracia A, Jéphos-Davennel C 2009 Microstructure evolution observation for SAC solder joint: Comparison between thermal cycling and thermal storage. Microelectronics Reliability 49: 1267–72
[18] Shnawah D A, Sabri M F, Badruddin I A 2012 A review on thermal cycling and drop impact reliability of SAC solder joint in portable electronic. Microelectronics Reliability 52(1):90-99
[19] Hammad A E 2013 Evolution of microstructure, thermal and creep properties of Ni-doped Sn–0.5Ag–0.7Cu low-Ag solder alloys for electronic applications. Materials and Design 52: 663-70
[20] Yoon J W, Chun H S, Koo J M, Lee H J, Jung S B 2007 Microstructural evolution of Sn-rich Au-Sn/Ni flip-chip solder joints under high temperature storage testing conditions. Scripta Mater; 56:661-4
[21] Lim G T, Kim B J, Lee K, Kim J, Joo Y C, Park Y B 2009 Effect of isothermal aging on intermetallic compounds and kirkendall void growth kinetics of Au stud bumps. Met Mater Int; 15:819-23
[22] Yu D Q, Oppermann H, Kleff J, Hutter M 2008 Interfacial metallurgical reaction between small flip-chip Sn/Au bumps and thin Au/TiW metallization under multiple reflow. Scripta Mater; 58:606-9
[23] Tang W, He A, Liu Q, Ivey D G 2008 Room temperature interfacial reactions in electrodeposited Au/Sn couples. Acta Mater 56:5818-27
[24] Li F Q, Wang C Q 2006 Influence of interfacial reaction between molten SnAgCu solder droplet and Au/Ni/Cu pad on IMC evolution. Transactions of Nonferrous Metals Society of China; 16: 18-22
[25] Lin C P, Chen C M 2012 Solid-state interfacial reactions at the solder joints employing Au/Pd/Ni and Au/Ni as the surface finish metallizations. Microelectronics Reliability 52: 385–390
[26] Dugal F, Ciappa M 2014 Study of thermal cycling and temperature aging on PbSnAg die attach solder joints for high power modules. Microelectronics Reliability; 54: 1856–6
[27] Chiu T C, Lin K L 2012 The growth of intermetallic compound in Cu/Sn3.5Ag/Au solder joints under current stressing. Intermetallics; 23: 208-216
[28] Chang C C, Wang Y W, Lai Y S, Kao C R 2010 Interfacial Reaction between 95Pb5Sn Solder Bump and 37Pb63Sn Presolder in Flip-Chip Solder Joints. Journal of Electronics Materials; 39: 1289-94
[29] Chang C W, Lee Q P, Ho C E, Kao C R 2006 Cross-interaction between Au and Cu in Au/Sn/Cu ternary diffusion couples. J Electronic Mater 35:366-71
[30] Yang L, Zhang Y C, Dai J, Jing Y F, Ge J G, Zhang N 2015 Microstructure, interfacial IMC and mechanical properties of Sn–0.7Cu–xAl (x = 0–0.075) lead-free solder alloy. Materials and Design; 67: 209-16
[31] Kanlayasiri K, Ariga T 2010 Influence of thermal aging on microhardness and microstructure of Sn–0.3Ag–0.7Cu–xIn lead-free solders. Journal of Alloys and Compounds; 504:L5-L9
[32] Anho¨ck S, Oppermann H, Kallmayer C, Aschenbrenner R, Thomas L, Reichl H 1998 in: Proceeding of the 1998 IEEE/CPMT Berlin International Electronics Manufacturing Technology Symposium, IEEE, Piscataway, NJ p. 156